Targeted inhibition of Snail family zinc finger transcription factors by oligonucleotide-Co(III) Schiff base conjugate

Allison S. Harney, Jiyoun Lee, Lisa M. Manus, Peijiao Wang, David M. Ballweg, Carole LaBonne[1], and Thomas J. Meade[1,2]

Departments of Chemistry, Biochemistry, Molecular and Cell Biology, Neurobiology and Physiology, and Radiology, Northwestern University, Evanston, IL 60208

Communicated by Brian M. Hoffman, Northwestern University, Evanston, IL, June 9, 2009 (received for review February 27, 2009)

A transition metal complex targeted for the inhibition of a subset of zinc finger transcription factors has been synthesized and tested in *Xenopus laevis*. A Co(III) Schiff base complex modified with a 17-bp DNA sequence is designed to selectively inhibit Snail family transcription factors. The oligonucleotide-conjugated Co(III) complex prevents Slug, Snail, and Sip1 from binding their DNA targets whereas other transcription factors are still able to interact with their target DNA. The attachment of the oligonucleotide to the Co(III) complex increases specificity 150-fold over the unconjugated complex. Studies demonstrate that neither the oligo, or the Co(III) Schiff base complex alone, are sufficient for inactivation of Slug at concentrations that the conjugated complex mediates inhibition. Slug, Snail, and Sip1 have been implicated in the regulation of epithelial-to-mesenchymal transition in development and cancer. A complex targeted to inactivate their transcriptional activity could prove valuable as an experimental tool and a cancer therapeutic.

gene expression | transition metal complex

Breast cancer is a heterogeneous disease with fatalities resulting from recurrence and metastasis to distant sites including bone, lung, liver, and brain (1). The zinc finger transcription factors Slug, Snail, and Sip1 have been implicated in tumor metastasis through the regulation of epithelial-to-mesenchymal transitions (EMTs) (2–5). Much of what is known about the molecular mechanism via which these transcriptional regulators mediate EMT are from developmental studies, particularly the induction of vertebrate neural crest migration (6–11). *Xenopus laevis* embryos have been used as a model system to study the molecular activities of Snail family members (9–12). During EMT, these transcriptional repressors down-regulate the expression of proteins involved in cell–cell adhesions characteristic of epithelial cells. Proteins involved in invasion, such as matrix metalloproteinases, are up-regulated, and cells lose their epithelial characteristics becoming invasive mesenchymal cells (2, 13–17).

Snail family transcription factors interact with DNA through zinc fingers of the C_2H_2 type with each finger coordinating 1 zinc ion (18). Slug and Snail are composed of 5 zinc fingers in tandem. Sip1 contains C-terminal and N-terminal zinc finger domains, each of which is composed of 3 tandem zinc fingers. Slug, Snail, and Sip1 bind to the Ebox consensus sequence CAGGTG in the promoter region of target genes with high specificity to mediate transcriptional repression. These transcription factors are emerging as targets for cancer therapeutics because of their role in EMT, and consequently, metastasis (19).

A zinc ion coordinated to 2 histidine and 2 cysteine residues is integral to the structure and function of zinc finger domains (20). It is well known that transition metals, such as Zn, Fe, and Co have a high affinity for histidines and cysteines. The affinity of the coordinated zinc for the histidine and cysteine residues has been used to generate transition metal inhibitors of enzymatic activity and DNA-protein interaction (21–24). Displacement of the zinc ion by a Co(III) Schiff base complex [Co(III)-sb] has been shown to inhibit DNA binding of at least 1 other zinc finger transcription factor (25) and enzymatic function of non-DNA binding proteins (25–28).

In the present study, oligonucleotide-linked Co(III)-sb with axial ammine ligands are used to target Ebox binding zinc finger domains and inhibit DNA binding (Fig. 1). The mechanism involves dissociative ligand exchange where the substitutionally active axial ammines are displaced by water to form the di-aquo species (28). The lone pair of electrons on the nitrogenous donors of the imidazole ring of histidines present in a zinc finger coordinate to the Co(III) agent irreversibly disrupting the coordination environment of Zn(II) (25, 27).

To target the Co(III)-sb to Snail family factors, and not other zinc-containing proteins, the acetyl acetonate ethylenediimine (acacen) backbone is linked to a modified oligonucleotide. This oligo contains the Ebox consensus sequence, CAGGTC, recognized by Snail factors (14). This modification does not alter the secondary structure of the DNA, enabling it to be readily coordinated by Snail proteins in a concentration dependent manner. The oligonucleotide confers DNA binding specificity such that only proteins that contain a zinc finger domain and bind the Ebox sequence are inhibited. A biochemical investigation of the functional role of the oligo and the Co(III) chelate of Co(III)-Ebox in the inhibition of DNA binding of Snail family transcription factors is presented using *X. laevis* as a model system. The specific inhibitory effects of Co(III)-Ebox for Slug, Snail, and Sip1 suggests that Co(III)-Ebox can be used as a tool to study EMT in vertebrate development and epithelial tumor metastasis (Fig. 1).

Results

Design and Synthesis of a Transcription Factor-Targeted Co(III)-sb. A Co(III)-sb conjugated to a DNA oligonucleotide that targets Ebox-binding zinc finger transcription factors was synthesized and characterized (Scheme 1). The Co(III) complex is prepared by the reaction of 6-heptenoic acid with sodium aizde and iodine monochloride to give 6-azido-7-iodo-heptanoic acid, compound 2, in 92% yield. The diazide, compound 3, was formed upon reaction of compound 2 with excess sodium azide in 23% yield. Compound 2 was reduced by hydrogenation to produce the diamine. Crude diamine was condensed with 2,4-pentadione to obtain the Schiff base ligand, compound 4, in 42% yield.

Author contributions: A.S.H., J.L., C.L., and T.J.M. designed research; A.S.H., J.L., L.M.M., P.W., and D.M.B. performed research; A.S.H. analyzed data; and A.S.H. and T.J.M. wrote the paper.

The authors declare no conflict of interest.

[1]C.L. and T.J.M. contributed equally to this work.

[2]To whom correspondence should be addressed. E-mail: tmeade@northwestern.edu.

This article contains supporting information online at www.pnas.org/cgi/content/full/0906423106/DCSupplemental.

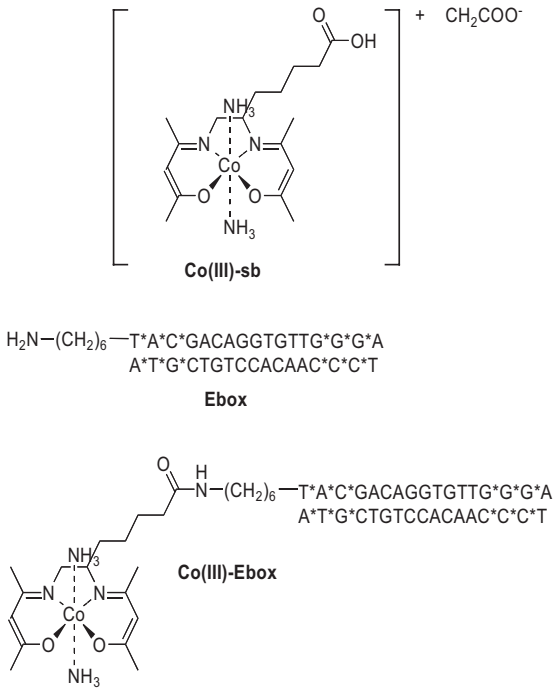

Fig. 1. Chemical structures of experimental complexes including Co(III) Schiff base complexes, Co(III)-sb and Co(III)-Ebox conjugate, and the duplex DNA Ebox.

Compound 4 was metallated using Co(II) acetate in methanol under a nitrogen atmosphere followed by bubbling ammonia into the reaction mixture to give Co(III)-sb (84%).

The Co(III)-sb was coupled to the oligonucleotide, Ebox (5′-T*A*C*GA**CAGGTG**TTG*G*G*A-3′), containing a 6-carbon amino-terminated linker at the 5′-end of one of the strands, containing 3 phosporothioate linkages at both the 3′ and 5′ ends of both strands. This modification prevents degradation by nucleases (as indicated by *, Ebox in bold). Co(III)-sb was coupled to the oligonucleotide using *N*,*N*′-dicyclohexyl carbodiimide (DCC) and NHS. The complementary strand of DNA was annealed by heating to 95 °C for 5 min and cooling slowly overnight. The resulting complex, Co(III)-Ebox, was purified using a Sephadex G-25 spin column and HPLC to yield 7.25 nmol (14.5%) of pure product (Fig. 1).

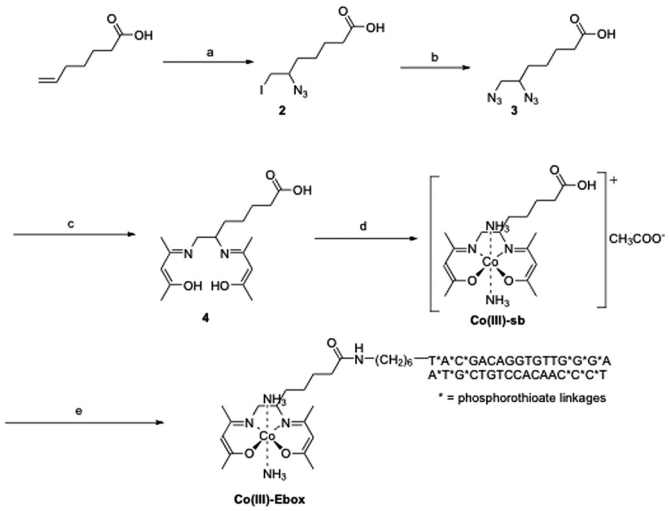

Scheme 1. Synthesis of the Co(III)-Ebox complex. (*A*) ICl, NaN_3, CH_3CN; 92% (*B*) NaN_3, DMF; 23% (*C*), compound 1. H_2, Pd/C, MeOh 2. 2,4-pentadione, MeOH:EtOH (2:3), 0 °C; 42% (*D*), compound 1. $Co(CH_3COO^-)_2 \cdot 4H_2O \cdot MeOH$, compound 2. NH_3 (g), 84% (*E*), compound 1. NHS, DCC, DMF, compound 2. 5′-amino-modified Ebox ssDNA, 100 mM MES, pH 6.0, compound 3. Complementary Ebox ssDNA 100 mM MES, pH 6.0, 95 °C, 14%.

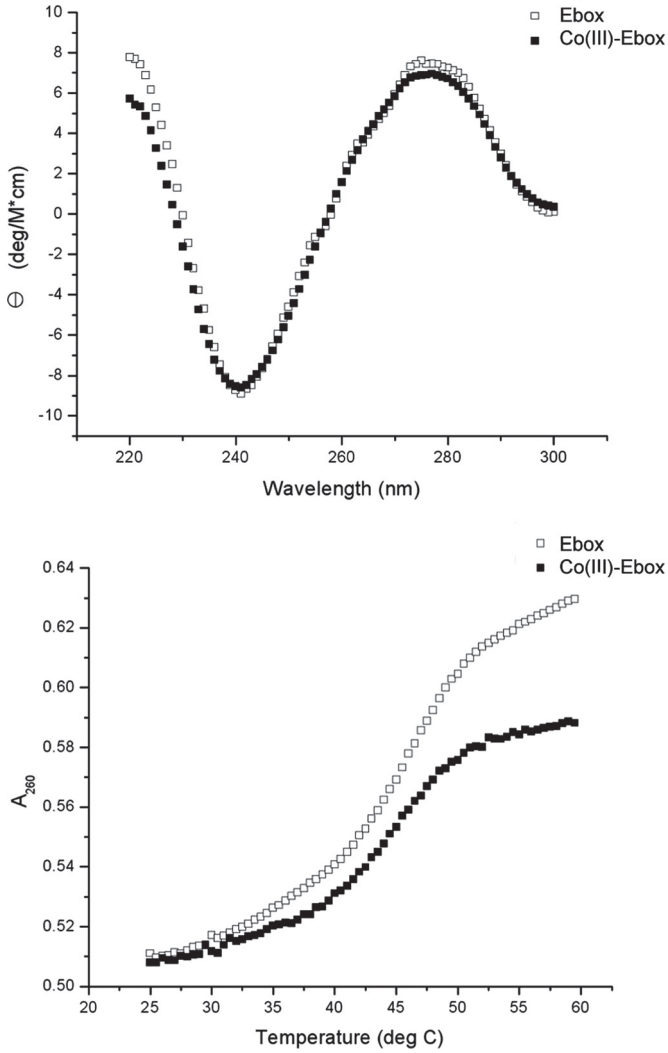

Fig. 2. Examination of the secondary structure of Co(III)-Ebox. (*A*) CD spectra at 25 °C of the Ebox (□) and Co(III)-Ebox (■) duplexes. Molar ellipticities, (Θ), are in units of deg/M·cm. Duplex concentrations are 1 μM in a 300 mM NaCl/20 mM PBS buffer solution, pH 7.0. (*B*) UV melting profiles at 260 nm for Ebox (□) and Co(III)-Ebox (■) duplexes at concentrations of 2 μM with a temperature range from 25 ° to 60 °C in a 0.1× SSC solution.

Duplex DNA Secondary Structure Evaluation. Native B-DNA conformation of the DNA is essential for a high affinity interaction between the oligonucleotide and the target protein. The secondary structure and strength of the duplex of Ebox and Co(III)-Ebox were examined by CD and melting profiles to ensure that modification with a metal chelate in Co(III)-Ebox has not altered the structure. CD in Fig. 2*A* shows the CD spectra for the modified oligonucleotide and the unmodified duplex DNA. The negative peak at 250 nm and the positive peak at 280 nm are characteristic of B-DNA (29, 30). These results indicate that the secondary structure of the oligonucleotide attached to Co(III)-Ebox is not altered as a result of the conjugation to a Co(III) chelate.

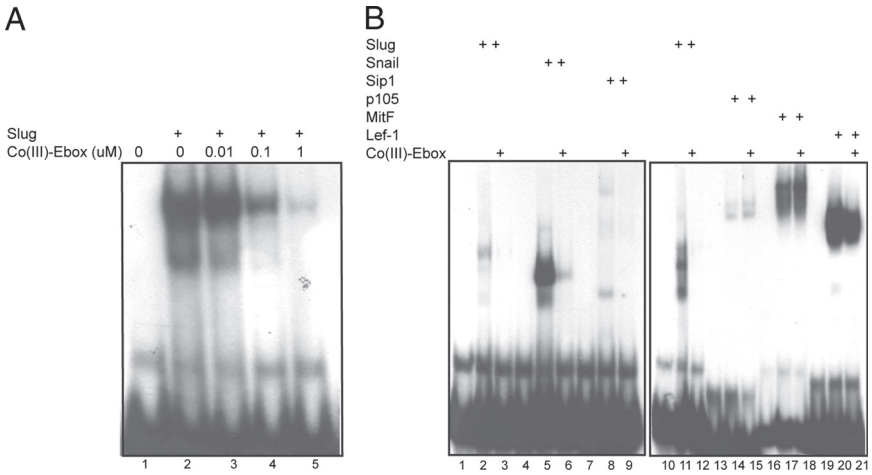

Fig. 3. Identification of Co(III)-Ebox targets. (*A*) Lysates of blastula stage embryos (lane 1) or embryos with overexpressed Slug protein (lanes 2–5) were incubated with increasing concentrations of Co(III)-Ebox of 0, 0.01, 0.1, and 1 μM for 15 min before challenge with a ^{32}P-labeled Ebox containing Slug DNA probe for 30 min. (*B*) Lysates of blastula stage embryos injected with Slug, Snail, or Sip1 mRNA (lanes 1–9) or Slug, p105, MitF, and Lef-1 mRNA (lanes 10–21) were incubated with 0 or 1 μM Co(III)-Ebox for 15 min before challenge with ^{32}P-labeled Slug probe for 30 min and analyzed by EMSA on a native gel. Lanes 1, 4, 7, 10, 13, 16, and 19 are uninjected control embryos incubated with the same labeled oligo as the lysates in the following 2 lanes to demonstrate a lack of nonspecific binding. Samples were analyzed by EMSA on a native TBE/acrylamide gel.

To further characterize the duplex DNA, melting points were determined using UV spectroscopy. Co(III)-Ebox DNA and unmodified Ebox DNA were heated in 0.1× SSC from 25.0 ° to 60.0 °C (Fig. 2*B*). The melting point for Ebox and Co(III)-Ebox were determined to be 46.0 ° and 44.7 °C, respectively. The similarity in the shape of the curve and the proximity of the melting points demonstrates that the DNA attached to Co(III)-Ebox maintains its native integrity, allowing the Co(III)-Ebox complex to selectively disrupt the function of its biological target.

Selectivity of Co(III)-Ebox for Slug, Snail, and Sip1. The oligonucleotide of Co(III)-Ebox contains an Ebox sequence, CAGGTG, designed to target the Snail family of transcription factors (Fig. 3). Investigation of the ability of Co(III)-Ebox to inhibit Slug was conducted by EMSA such that the concentration of Co(III)-Ebox added to each sample was increased (Fig. 3*A*). Partial inhibition of DN binding was achieved at 100 nM and complete inhibition of DNA binding at 1 μM. Slug, Snail, and Sip1 have been implicated in having a role in EMT during metastatic progression of epithelial tumors. That Co(III)-Ebox interacts with 3 of the transcription factors involved in EMT is advantageous because it eliminates the response to more than one molecular mediator of the process (Fig. 3*B*).

We have found that the function of zinc fingers is inhibited by Co(III)-sb via a dissociative ligand exchange mechanism because Co(III) has high affinity toward the nitrogen in the imidazole ring of a histidine residue in the zinc finger (25). The ligand exchange is on the axial ligands, because a Co(III)-sb with substitutionally labile 2-methyl imidazole axial ligands irreversibly interacts with a model zinc finger peptide whereas a substitutionally inert Co(III)-sb with imidizole axial ligands does not (27). This is an irreversible reaction, and inhibition of DNA binding is concentration dependent.

To demonstrate that Co(III)-Ebox-mediated inhibition of DNA binding is irreversible and not simply due to competition by the Ebox target sequence in the zinc finger region, we have determined the percentage of shifted Slug protein that has been irreversibly modified by Co(III)-Ebox and can no longer be competed by unlabeled Ebox oligo. Whole embryo lysates expressing Slug were preincubated with 5 nM radiolabeled Co(III)-Ebox or Ebox (Fig. 4, lanes 2–6 and lanes 8–12). As increasing concentrations of unlabeled Ebox was added to the lysates, the radiolabeled Ebox bound to Slug was displaced. The signal decreased to baseline, as compared with the uninjected lane (Fig. 4, lane 12). At 100-fold excess unlabeled Ebox over the radiolabeled probe, the residual Ebox bound to Slug is $-5.9 \pm 0.8\%$. Comparatively, $28.5 \pm 3.3\%$ of Co(III)-Ebox labeled Slug at 100-fold excess unlabeled Ebox (Fig. 4, lane 6). This is the percentage of Co(III)-Ebox that has irreversibly modified Slug through the interaction with the Co(III) metal center. These

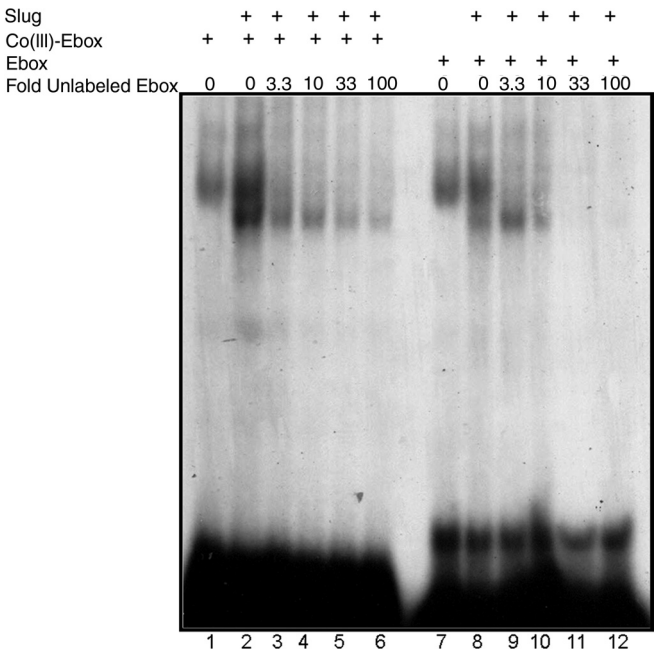

Fig. 4. Co(III)-Ebox irreversibly binds Slug through the Co(III)-sb. Lysates of blastula stage embryos injected with Slug mRNA were incubated with ^{32}P-labeled Co(III)-Ebox (lanes 2–6) or ^{32}P-labeled Ebox (lanes 8–12) for 75 min. Bound complexes were challenged with increasing concentrations of unlabeled Ebox of 0-, 3.3-, 10-, 33-, and 100-fold excess over labeled compound concentrations (lanes 3–6 and lanes 9–12) and incubated for 75 min. The interaction complexes were visualized by EMSA and quantified by PhosphorImager. Uninjected embryos are presented in lanes 1 and 7.

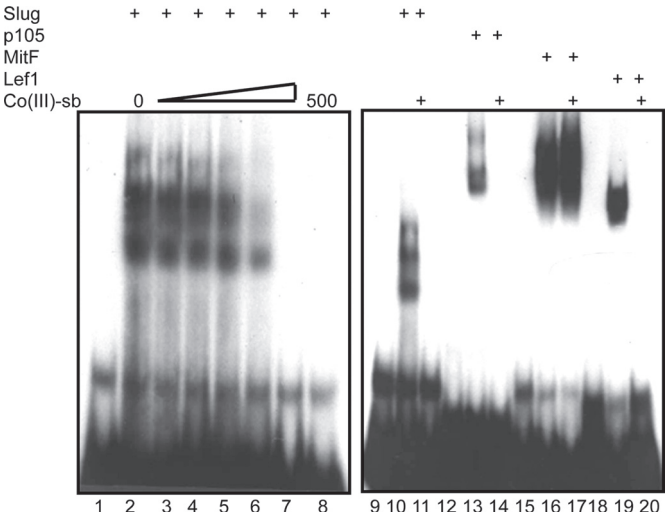

Fig. 5. DNA-mediated binding selectivity. Lysates of blastula stage embryos injected with Slug mRNA were incubated with increasing concentrations of Co(III)-sb of 0, 1.5, 5, 15, 50, 150, and 500 μM (lanes 2–8) for 15 min, then incubated with ^{32}P-labeled Slug probe for 30 min and visualized by EMSA. Lysates of embryos injected with Slug (lanes 10 and 11), p105 (lanes 13 and 14), MitF (lanes 16 and 17), or Lef-1 (lanes 19 and 20) mRNA were incubated with 0 or 150 μM Co(III)-sb for 15 min and labeled with ^{32}P-labeled Slug probe for 30 min. Uninjected embryos are presented in lanes 1, 9, 12, 15, and 18. Samples were separated by EMSA.

results confirm that Co(III)-Ebox interacts with Slug, deactivating the zinc finger region and inhibiting the proteins' ability to bind DNA.

To verify specificity of this interaction, transcription factors that could be inhibited by the Co(III)-sb, the oligo alone, or by nonspecific interactions were also examined. p105 contains a zinc finger region that could interact with untargeted Co(III)-sb (31). MitF is a bHLH protein that can bind the Ebox consensus sequence and could therefore be inhibited by excess oligo (32). Lef-1 contains neither a zinc finger region nor specificity for Eboxes and is used to verify that the effects are not due to surface interactions or other nonspecific binding (33).

Although Co(III)-Ebox inhibits Slug, Snail, and Sip1 at 1 μM incubation concentration, p105, MitF, and Lef-1 were not inhibited (Fig. 3*B*). The protein expression levels in the whole embryo lysates for these transcription factors is equal as seen by western blot (Fig. S1). The difference in band intensity can be attributed to a difference in binding affinity to the target oligo. These results reveal effective targeting of Co(III)-Ebox to Snail family members with no off-target effects. Effective inhibition requires both a zinc finger region in the protein for interaction with the Co(III) metal and binding to the Ebox sequence that will bind to the oligonucleotide. For the complex to be an effective experimental or therapeutic tool, it should have high specificity for target factors to avoid off-target effects, as Co(III)-Ebox has for Slug, Snail, and Sip1.

Examination of Selectivity of Co(III)-sb Inhibition. In the absence of a targeting moiety, such as an oligonucleotide, we have reported that multiple cobalt complexes can interact with a single protein, although only 1 is required for complete inhibition of function (25, 27, 28). To examine the effectiveness of targeting, the minimal concentration at which Co(III)-sb inhibits Slug DNA binding was determined. The Co(III)-sb complex requires 150-fold excess to achieve comparable inhibition of Slug to that achieved by Co(III)-Ebox at 1 μM (Fig. 5). When DNA binding by p105 and Lef-1 is inhibited, MitF is not (Fig. 5). By contrast, 1 μM Co(III)-Ebox is sufficient for inhibition of Slug, Snail, and Sip1, but does not inhibit transcription factors that are not targeted by the Ebox moiety (Fig. 3*B*). Unsurprisingly, at high concentrations Co(III)-sb can inhibit p105 and Lef-1, because both factors contain amino acid residues in the DNA binding region with electron-donating atoms that can coordinately bond to Co(III)-sb to alter the protein structure. In p105, there are both cysteine and histidine residues in the zinc finger regions that have an affinity for Co(III) (34). Similarly, Lef-1 contains a methionine residue at position 13 important for intercalation into DNA (33). Because the interaction of Lef-1 with DNA is disrupted by Co(III)-sb, it is postulated that the interaction of Co(III)-sb with the sulfur group causes disruption of DNA binding.

Conclusions

Transcription factors involved in misregulation of gene expression leading to disease are potential targets of therapeutic agents. We have developed a Co(III)-sb and conjugated the complex to an Ebox-containing oligonucleotide, Co(III)-Ebox, for inactivation of Snail family factors. We have successfully demonstrated the specificity of Co(III)-Ebox for selective inhibition of Slug, Snail, and Sip1. The Co(III)-Ebox complex was designed to irreversibly bind zinc finger transcription factors through a ligand exchange mechanism on Co(III), and is targeted to Snail family transcription factors through an Ebox consensus sequence in the oligo. The Co(III)-sb is attached to the targeting oligonucleotide through a short linker. Together, Co(III)-sb and Ebox, as two components of Co(III)-Ebox, mediate precise inhibition of target zinc finger proteins, where the target protein must bind the target DNA. In the absence of the oligonucleotide, >100-fold more Co(III)-sb are required for Slug inhibition. At this same concentration, Co(III)-sb interacts nonspecifically with other proteins. In *X. laevis* embryos, Slug inhibition is conferred by Co(III)-Ebox whereas neither Ebox nor Co(III)-sb are sufficient for irreversible Slug inhibition at the same concentration. This specificity of action and the lack of off-target effects suggests that Co(III)-Ebox can have specific effects on migratory cell populations, including the neural crest and metastatic cancers, while minimizing toxicity.

Materials and Methods

General Synthesis Methods. Unless noted, materials and solvents were purchased from Sigma–Aldrich and used without further purification. Acetonitrile was purified using a Glass Contour Solvent System. Deionized water was obtained from a Millipore Q-Guard System equipped with a quantum Ex cartridge. Cobalt(II) acetate tetrahydrate was purchased from EM Science. Unless noted, all syntheses were performed under a nitrogen atmosphere. TLC was carried out on 60F 254 silica gel plates (EMD Biosciences). Visualization was accomplished by UV light, CAM stain, or bromocresol green stain. Flash column chromatography was executed with standard grade 60 Å 230–400 mesh silica gel (Sorbent Technologies). Desalting columns, Accubond II ODS-C18 cartridges, were purchased from Agilent Technologies.

^{1}H and ^{13}C NMR spectra were either obtained on a Bruker 600 MHz Avance III NMR Spectrometer or a Bruker 500MHz Avance III NMR Spectrometer with deuterated solvent as noted. High-resolution electron ionization mass spectra were obtained on an Agilent 6210 LC-TOF with Agilent 1200 HPLC introduction (Agilent Technologies). UV-visible spectroscopy was carried out on an Agilent 8453 diode array spectrometer (Agilent Technologies). HPLC purification was performed on a Varian Prostar 500 (for analysis) system with a semipreparative Dionex DNAPac PA 100 column (9 $\times$ 250 mm). The mobile phase consisted of 1.5 M NH_4Cl with 20 mM Tris buffer in 0.5% CH_3CN, pH 8.0 (solvent A), and 20 mM Tris buffer in 0.5% CH_3CN, pH 8.0 (solvent B). Hydrogenation was performed on a Parr shaker hydrogenation apparatus. Mass spectrometry measurements of the final complex were performed with matrix-assisted laser desorption ionization time of flight (MALDI-TOF) mass spectrometry on a Perseptive Biosystems Voyager ProDE spectrometer using a 2,4,6-trihydroxyacetophenone (THAP)/ammonium citrate matrix, calibrated by standard polythymine oligonucleotides. Elemental analysis was preformed by QTI Intertek USA. Inductively coupled plasma mass spectrometry (ICP-MS) measurements were obtained on an X Series ICP-MS (Thermo Scientific).

6-Azido-7-Iodo-Heptanoic Acid (Compound 2). Diluted in 15 mL acetonitrile, iodine monochloride (0.74 mL, 14.8 mmol) was added via addition funnel to a suspension of sodium azide (1.912 g, 29.5 mmol) in 10 mL acetonitrile at 0 °C over 20 min, with stirring. Upon complete addition, the reaction mixture was allowed to warm to room temperature. Six-heptenoic acid (1.00 mL, 7.38 mmol) in 5 mL acetonitrile was added dropwise to the reaction mixture via addition funnel. The resultant reaction mixture was allowed to stir at room temperature overnight. Absence of starting material was confirmed via TLC analysis. The reaction mixture was diluted with water, and the organic layers were extracted with diethyl ether. The combined organic layers were washed with 5% sodium thiosulfate in water, dried over $MgSO_4$, and concentrated under reduced pressure. The resultant light pink crude material was purified by flash column chromatography over silica gel with toluene:ether:acetic acid (63:35:2) to give a pale yellow oil (1.999 g, 91%). ^{1}H NMR (600 MHz, $CDCl_3$) δ 3.41 (dd, J = 10.6, 16.5, 1H), 3.26 (d, J = 5.7, 2H), 2.40 (t, 2H), 1.83–1.37 (m, 6H). ^{13}C NMR (151 MHz, $CDCl_3$) δ 179.62, 62.45, 34.12, 33.73, 25.26, 24.17, 8.21. Analysis calculated (Anal. Calcd.) for compound 2: C, 28.30; H, 4.07; N, 14.14. Found: C, 28.43; H, 4.12; N, 14.80.

6,7-Diazido-Heptanoic Acid (Compound 3). Sodium azide (0.765 g, 11.8 mmol) and compound 2 (1.556 g, 5.24 mmol) were combined in the presence of 10 mL *N*,*N*′-dimethylformamide (DMF). The reaction mixture was stirred at 55 °C overnight. The reaction mixture was diluted with water and the organic layers extracted with diethyl ether. The combined organic layers were washed with water, dried over $MgSO_4$, and concentrated under reduced pressure. The crude product was purified by flash column chromatography over silica gel with ethyl acetate:hexanes (3:2) to afford a light yellow oil (0.253 g, 23%). ^{1}H NMR (500 MHz, $CDCl_3$) δ 3.61–3.23 (m, 3H), 2.40 (t, J = 7.0, 2H), 1.77–1.36 (m, 6H). ^{13}C NMR (126 MHz, $CDCl_3$) δ 179.36, 61.79, 54.80, 33.64, 31.45, 25.33, 24.24. Electrospray ionization mass spectrometry (ESI-MS) (*m/z*) $C_7H_{12}N_2O_2$ $[M\text{-}H]^-$: Calc. 211.0960, found 211.09504.

(Heptanoic Acido)(Acacen) [6,7-Bis(2-Imino-4-Oxopentyl)Heptanoic Acid] (Compound 4). Compound 3 (1.094 g, 5.16 mmol) in methanol under nitrogen bubbling was combined with an equal amount of palladium on carbon (10% by weight) and hydrogenated at 45 psi overnight. The resultant material was filtered through celite with methanol and concentrated under reduced pressure (0.676 g, 82%). Without further purification, the diamine (1.148 g, 7.16 mmol) was dissolved in 15 mL methanol:ethanol (2:3) and slowly added via addition funnel to a 15-mL solution of 2,4-pentadione (7.4 mL, 71.8 mmol) in methanol:ethanol (2:3) with vigorous stirring at 0 °C. Immediately after addition, the resultant yellow mixture was concentrated under reduced pressure to give a yellow solid. This crude material was recrystalized in hot toluene to give a white crystalline solid (0.984 g, 42%). ^{1}H NMR (600 MHz, $CDCl_3$) δ 11.00 (s, 1H), 10.89 (d, J = 10.1, 1H), 4.97 (s, 1H), 4.95 (s, 1H), 3.61 (bs, 1H), 3.36–3.26 (m, 2H), 2.34 (dd, J = 7.0, 13.9, 2H), 2.00 (s, 6H), 1.87 (d, J = 15.1, 6H), 1.70–1.37 (m, 6H). ^{13}C NMR (151 MHz, $CDCl_3$) δ 195.36, 195.26, 176.16, 163.77, 163.48, 96.11, 96.02, 54.29, 48.70, 33.72, 33.02, 28.71, 28.64, 25.29, 24.49, 19.05, 18.75. ESI-MS (*m/z*) $C_{17}H_{27}N_2O_4$ $[M\text{-}H]^-$: Calc. 323.1976, found 323.19764. Anal. Calcd. for compound 4: C, 62.94; H, 8.70; N, 8.64. Found: C, 63.12; H, 8.67; N, 8.53.

[Co(III)(Heptanoic Acido)(Acacen)$(NH_3)_2]^+CH_3COO^-$ [Co(III)-sb]. Cobalt acetate (0.182 g, 0.732 mmol) was dissolved in 5 mL methanol and filtered whereas compound 4 (0.238 g, 0.733 mmol) was dissolved separately in 5 mL methanol. Nitrogen was bubbled through the reagent solutions for 15 min. Under nitrogen, the cobalt acetate solution was added dropwise to compound 4, resulting in an instantaneous orange-brown color. The solution was allowed to stir for 1 h. The reaction was opened to air, and ammonia was bubbled through into the solution for 1 h, followed by concentration under reduced pressure. The compound was used without further purification (0.255 g, 84%). ^{1}H NMR (500 MHz, MeOD) δ 3.60 (m, 2H), 3.25 (s, 1H), 2.16 (d, J = 6.1, 8H), 2.01 (d, J = 6.6, 6H), 1.84 (m, 6H). The vinyl protons were obscured by the solvent peak. Small impurities were detected at 2.56 and 2.28 ppm. ^{13}C NMR (126 MHz, MeOD) δ 179.33, 178.54, 171.40, 170.30, 166.46, 97.63, 96.74, 64.80, 57.28, 35.68, 28.45, 25.47, 25.41, 22.58, 22.38, 19.38, 18.93. Small impurities were detected at 49.91 and 29.10 ppm.

Co(III)-Oligonucleotide Conjugate [Co(III)-Ebox]. 5′-Amino-modified DNA (2.33 μmol) and the unmodified complementary strand (2.0 μmol) were purchased from IDT DNA. Each of the complementary DNA strands was suspended in 100 mM Mes buffer (pH 6.0, 1 mL). A solution of Co(III)-sb (2.49 mg, 6.0 μmol) and NHS (4.14 mg, 36 μmol) in 200 μL DMF was treated with DCC (7.43 mg, 36 μmol). The reaction mixture was stirred at room temperature for 1 h. The reaction was monitored by ESI-MS to confirm the formation of activated ester of Co(III)-sb. The reaction mixture was added to 260 μL solution of 50 nmol 5′-amino-modified DNA and stirred at room temperature for 24 h. To this solution, 50 nmol of the complementary strand was added, and the mixture was heated to 95 °C for 5 min and cooled slowly overnight. The mixture was purified by Microspin G-50 to remove excess amount of Co(III)-sb and other coupling reagents and freeze-dried. The crude residue was further purified by anion-exchange HPLC on a semipreparative Dionex DNAPac PA100 column (9 × 250 mm), 10%–60% buffer A (1.5 M NH_4Cl, 20 mM Tris, 0.5% CH_3CN, pH 8.0) into buffer B (20 mM Tris, 0.5% CH_3CN, pH 8.0) solution over 40 min. Co(III)-Ebox was identified by its absorbance at 260 nm with visible bands because of the metal-to-ligand charge transfer (MLCT) states of the cobalt complex at 336 nm. The retention time of Co(III)-Ebox was ≈27 min. After HPLC purification and lyophilization, the fractions containing Co(III)-Ebox were desalted and eluted with 60% MeOH/water. The concentration of the conjugate was determined by calculating the Co(III) concentration by ICP-MS (14.5%) and verified by the absorbance of DNA at 260 nm. MALDI-TOF Co(III)-Ebox calculated: [M]/4: 2783.7, found: 2738.9.

CD Spectroscopy. CD measurements were performed on a Jasco Model J-715 spectrometer with 150 W air-cooled Xenon lamp as light source. CD spectra were collected at 25 °C in a 1-cm-path-length cell at band width 1 nm, data pitch 0.2 nm, and response time of 2 s. The concentrations of Co(III)-Ebox and Slug control were 1 μM in 300 mM NaCl/20 mM PBS buffer solutions (pH 7.0).

Thermal Denaturation. T_m measurements were acquired at 260 nm on an Agilent 8453 UV-visible spectrophotometer (Agilent Technologies) with a 1-cm optical path length. The temperature was increased by increments of 0.5 °C by a Peltier temperature controller, with a hold time of 1 min. Measurements were acquired in a solution of 0.1× SSC (150 mM NaCl, 15 mM NaCitrate), with a duplex concentration of 2 μM. The T_m for each of the duplexes was determined as the first integral of the curve.

Embryo Preparation and Constructs. Pigmented and albino eggs were obtained and fertilized using standard protocols (35). All embryos are staged using the Niewenkoop–Faber method. Embryos were injected into 1 cell at stage 1 in 0.4× MMR (Marc's modified ringer's solution) with 3% Ficoll then transferred to 0.1× MMR until harvesting. mRNA was transcribed in vitro using the SP6 Message Machine kit (Ambion). Concentrations of mRNA injected into 1 cell at the 2-cell stage range from 5–50 pg. XSip1 in the vector pCS2+ was obtained from A. Eisaki (36). cDNA was generated using PCR amplification and a high fidelity polymerase (Pfu; Roche). cDNAs were cloned into a pCS2 variant that adds 5 myc tags to either the N or C terminus. All constructs were confirmed by sequencing using a ABI 3730 high-throughput DNA Sequencer (Applied Biosystems).

Electrophoretic Mobility Shift Assays. To radiolabel oligonucleotide targets, 1.25 pmol annealed oligonucleotide (IDT DNA) was labeled at the 5′ end with [^{32}]ATP (Amersham) by T4 polynucleotide kinase according to the manufacturer's protocol (Gibco BRL Life Technologies). Free nucleotides were removed using ProbeQuant G-50 micro columns (GE Healthcare). The duplex oligonucleotide sequences used are as follows:

Slug: 5′-TGTTTCCATCCCAACACCTGTCGTATACAA-3′
Lef-1 (37): 5′-TCGAATTCTCACCCTTTGAAGCTCTT-3′
NF-κB (Promega): 5′-GCCTGGGAAAGTCCCCTCAACT-3′
MitF: 5′-CAGGTG-3′

For in vitro assays, whole embryo lysates were prepared by lysing 5 stage-8 embryos in 100 μL lysis buffer (1× PBS, 1% Nonidet P-40, and Complete Protease Inhibitor Mixture Tablets; Roche). In the EMSA, 5 μL embryo lysate were combined with 25 μg/mL poly-dI/dC (Sigma), 5 μL EMSA binding buffer (20 mM Hepes, pH 7.6, 150 mM KCl, 3 mM $MgCl_2$, 0.5 mg/mL BSA, 10% glycerol, and 0.2 mM $ZnSO_4$), and indicated amounts of Co(III)-Ebox that were incubated at room temperature for 15 min. After the incubation, 2 μL radiolabeled oligonucleotide probe were added and incubated at room temperature for an additional 30 min. Protein-DNA complexes were resolved on a 5% TBE/acrylamide gel.

To determine irreversibility, embryos were injected with Slug mRNA, and embryos were collected after 6 h of incubation at 18 °C and lysed as above. The EMSA binding reaction used 5 μL lysate combined with 25 μg/mL poly-dI/dC, 5 μL EMSA binding buffer, and 0.1 pmol (final concentration of 5 nM) ^{32}P-labeled Co(III)-Ebox or Ebox. Binding reactions were incubated at room temperature for 75 min. Unlabeled Ebox oligonucleotide was subsequently added at 0-, 3.3-, 10-, 33-, and 100-fold excess over the preincubation concentration of radiolabeled Co(III)-Ebox and Ebox. Complexes were incubated at room temperature for 75 min. Protein-DNA complexes were resolved on a 5% TBE/acrylamide gel. This experiment was performed in triplicate. Fig. 4 is a representative image of one replicate.

Band intensities were quantified on a PhosphorImager. Slug-bound band intensity values were background-subtracted using the uninjected lane and normalized to the background signal in each individual lane. The percentage of residual complex bound to Slug is the normalized intensity at 100-fold excess unlabeled Ebox divided by the normalized intensity in the lane where no competitor was added. These values for Co(III)-Ebox and Ebox were averaged over three replicates and reported with the standard error.

The presence of 3 shifted complexes for Slug have been reported (38). Co(III)-Ebox inhibits all of the complexes as seen in Figs. 3, 4, and 5.

Western Blot Analysis. For Western blots, embryo lysates from EMSA were used. Samples were denatured and resolved on SDS/PAGE. Proteins were detected using antibodies against the myc epitope tag (Myc: 9E10; Santa Cruz Biotechnology).

ACKNOWLEDGMENTS. The authors thank A. Eisaki [Department of Life Sciences (Biology), Core Research of Evolutional Sciences and Technology, Japan Science and Technology Corporation, University of Tokyo, Tokyo, Japan] for providing reagents and D. Mastarone for aid with NMR characterization. This work is supported by Nanomaterials for Cancer Diagnostics and Therapeutics Grant 5 U54 CA1193 41–02 and the Rosenberg Cancer Foundation. A.S.H. is supported by the Natural Sciences and Engineering Research Council of Canada graduate fellowship.

1. Kuperwasser C, et al. (2005) A mouse model of human breast cancer metastasis to human bone. *Cancer Res* 65:6130–6138.
2. Savagner P, Yamada KM, Thiery JP (1997) The zinc-finger protein slug causes desmosome dissociation, an initial and necessary step for growth factor-induced epithelial-mesenchymal transition. *J Cell Biol* 137:1403–1419.
3. Vandewalle C, et al. (2005) SIP1/ZEB2 induces EMT by repressing genes of different epithelial cell-cell junctions. *Nucleic Acids Res* 33:6566–6578.
4. Kuphal S, Palm HG, Poser I, Bosserhoff AK (2005) Snail-regulated genes in malignant melanoma. *Melanoma Res* 15:305–313.
5. Blanco MJ, et al. (2002) Correlation of Snail expression with histological grade and lymph node status in breast carcinomas. *Oncogene* 21:3241–3246.
6. Sakai D, Suzuki T, Osumi N, Wakamatsu Y (2006) Cooperative action of Sox9, Snail2 and PKA signaling in early neural crest development. *Development* 133:1323–1333.
7. Cheung M, et al. (2005) The transcriptional control of trunk neural crest induction, survival, and delamination. *Dev Cell* 8:179–192.
8. Mayor R, Morgan R, Sargent MG (1995) Induction of the prospective neural crest of *Xenopus*. *Development* 121:767–777.
9. Aybar MJ, Nieto MA, Mayor R (2003) Snail precedes slug in the genetic cascade required for the specification and migration of the *Xenopus* neural crest. *Development* 130:483–494.
10. LaBonne C, Bronner-Fraser M (2000) Snail-related transcriptional repressors are required in *Xenopus* for both the induction of the neural crest and its subsequent migration. *Dev Biol* 221:195–205.
11. Carl TF, Dufton C, Hanken J, Klymkowsky MW (1999) Inhibition of neural crest migration in *Xenopus* using antisense slug RNA. *Dev Biol* 213:101–115.
12. Vernon AE, Labonne C (2006) Slug stability is dynamically regulated during neural crest development by the F-box protein Ppa. *Development* 133:3359–3370.
13. Shiozaki H, Oka H, Inoue M, Tamura S, Monden M (1996) E-cadherin mediated adhesion system in cancer cells. *Cancer* 77(8 Suppl):1605–1613.
14. Martinez-Estrada OM, et al. (2006) The transcription factors Slug and Snail act as repressors of Claudin-1 expression in epithelial cells. *Biochem J* 394:449–457.
15. Peinado H, Ballestar E, Esteller M, Cano A (2004) Snail mediates E-cadherin repression by the recruitment of the Sin3A/histone deacetylase 1 (HDAC1)/HDAC2 complex. *Mol Cell Biol* 24:306–319.
16. Yang Z, et al. (2005) Pak1 phosphorylation of snail, a master regulator of epithelial-to-mesenchyme transition, modulates snail's subcellular localization and functions. *Cancer Res* 65:3179–3184.
17. Peinado H, Portillo F, Cano A (2004) Transcriptional regulation of cadherins during development and carcinogenesis. *Int J Dev Biol* 48:365–375.
18. Papworth M, et al. (2003) Inhibition of herpes simplex virus 1 gene expression by designer zinc-finger transcription factors. *Proc Natl Acad Sci USA* 100:1621–1626.
19. Weinstein IB, Joe AK (2006) Mechanisms of disease: Oncogene addiction—A rationale for molecular targeting in cancer therapy. *Nat Clin Pract Oncol* 3:448–457.
20. Hartwig A (2001) Zinc finger proteins as potential targets for toxic metal ions: Differential effects on structure and function. *Antioxid Redox Signal* 3:625–634.
21. Epstein SP, et al. (2006) Efficacy of topical cobalt chelate CTC-96 against adenovirus in a cell culture model and against adenovirus keratoconjunctivitis in a rabbit model. *BMC Ophthalmol* 6:22.
22. Schwartz JA, Lium EK, Silverstein SJ (2001) Herpes simplex virus type 1 entry is inhibited by the cobalt chelate complex CTC-96. *J Virol* 75:4117–4128.
23. Larabee JL, Hocker JR, Hanas JS (2005) Mechanisms of aurothiomalate-Cys2His2 zinc finger interactions. *Chem Res Toxicol* 18:1943–1954.
24. Watkin RD, Nawrot T, Potts RJ, Hart BA (2003) Mechanisms regulating the cadmium-mediated suppression of Sp1 transcription factor activity in alveolar epithelial cells. *Toxicology* 184:157–178.
25. Louie AY, Meade TJ (1998) A cobalt complex that selectively disrupts the structure and function of zinc fingers. *Proc Natl Acad Sci USA* 95:6663–6668.
26. Bottcher ATT, Hardcastle K, Meade T, Gray H (1997) Spectroscopy and electrochemistry of cobalt(III) Schiff base complexes. *Inorg Chem* 36:2498–2504.
27. Takeuchi T, Bottcher A, Quezada CM, Meade TJ, Gray HB (1999) Inhibition of thermolysin and human alpha-thrombin by cobalt(III) Schiff base complexes. *Bioorg Med Chem* 7:815–819.
28. Blum O, et al. (1998) Isolation of a myoglobin molten globule by selective cobalt(III)-induced unfolding. *Proc Natl Acad Sci USA* 95:6659–6662.
29. Gray DM, Ratliff RL, Vaughan MR (1992) Circular dichroism spectroscopy of DNA. *Methods Enzymol* 211:389–406.
30. Bush C (1974) *Basic Principles in Nucleic Acid Chemistry*, ed Ts'o POP (Academic, New York).
31. Zabel U, Schreck R, Baeuerle PA (1991) DNA binding of purified transcription factor NF-kappa B. Affinity, specificity, Zn2+ dependence, and differential half-site recognition. *J Biol Chem* 266:252–260.
32. Goding CR (2000) Mitf from neural crest to melanoma: Signal transduction and transcription in the melanocyte lineage. *Genes Dev* 14:1712–1728.
33. Balaeff A, Churchill ME, Schulten K (1998) Structure prediction of a complex between the chromosomal protein HMG-D and DNA. *Proteins* 30:113–135.
34. Toledano MB, Ghosh D, Trinh F, Leonard WJ (1993) N-terminal DNA-binding domains contribute to differential DNA-binding specificities of NF-kappa B p50 and p65. *Mol Cell Biol* 13:852–860.
35. Bellmeyer A, Krase J, Lindgren J, LaBonne C (2003) The protooncogene c-myc is an essential regulator of neural crest formation in *Xenopus*. *Dev Cell* 4:827–839.
36. Eisaki A, Kuroda H, Fukui A, Asashima M (2000) XSIP1, a member of two-handed zinc finger proteins, induced anterior neural markers in *Xenopus laevis* animal cap. *Biochem Biophys Res Commun* 271:151–157.
37. Vallin J, et al. (2001) Cloning and characterization of three *Xenopus* slug promoters reveal direct regulation by Lef/beta-catenin signaling. *J Biol Chem* 276:30350–30358.
38. Bolos V, et al. (2003) The transcription factor Slug represses E-cadherin expression and induces epithelial to mesenchymal transitions: A comparison with Snail and E47 repressors. *J Cell Sci* 116:499–511.